Published in final edited form as:
Circ Arrhythm Electrophysiol. 2012 December ; 5(6): 1160–1167. doi:10.1161/CIRCEP.111.969519.

Long-Term Frequency Gradients during Persistent Atrial Fibrillation in Sheep are Associated with Stable Sources in the Left Atrium

David Filgueiras-Rama, MD[1,*], **Nicholas F. Price, MSc**[1,2,*], **Raphael P. Martins, MD**[1], **Masatoshi Yamazaki, MD**[1], **Uma Mahesh R. Avula, MD**[1], **Kuljeet Kaur, PhD**[1], **Jérôme Kalifa, MD**[1], **Steven R. Ennis, PhD**[1], **Elliot Hwang, BSE**[1], **Vijay Devabhaktuni, PhD**[2], **Jose Jalife, MD**[1,3], and **PhD Omer Berenfeld**[1,4]

[1]Center for Arrhythmia Research, Dept of Internal Medicine

[3]Dept of Molecular & Integrative Physiology

[4]Dept of Biomedical Engineering, University of Michigan. Ann Arbor, MI

[2]Dept of Electrical Engineering and Computer Science, College of Engineering, University of Toledo, Toledo, OH

Abstract

Background—Dominant frequencies (DFs) of activation are higher in the atria of patients with persistent than paroxysmal atrial fibrillation (AF) and left-to-right atrial (LA-to-RA) DF gradients have been identified in both. However, whether such gradients are maintained as long-term persistent AF is established remains unexplored. We aimed at determining *in-vivo* the time-course in atrial DF values from paroxysmal to persistent AF in sheep, and test the hypothesis that a LA-to-RA DF difference is associated with LA drivers in persistent AF.

Methods and Results—AF was induced using RA tachypacing (N=8). Electrograms were obtained weekly from a RA lead and a loop recorder (ILR) implanted near the LA. DFs were determined for 5-sec-long electrograms (QRST subtracted) during AF in-vivo and in ex-vivo optical mapping. Underlying structural changes were compared to weight-matched controls (N=4). Following the first AF episode, DF increased gradually over a 2-week period (7±0.21 to 9.92±0.31 Hz, N=6, $p<0.05$). During 9–24 weeks of AF the DF values on the ILR were higher than the RA (10.6±0.08 vs. 9.3±0.1 Hz, respectively; N=7, $p<0.0001$). Subsequent optical mapping confirmed a DF gradient from posterior LA-to-RA (9.1±1.0 to 6.9±0.9 Hz. $p<0.05$) and demonstrated patterns of activation compatible with drifting rotors in the posterior LA (PLA). Persistent AF sheep showed significant enlargement of the PLA compared to controls.

Correspondence: Omer Berenfeld, PhD Center for Arrhythmia Research University of Michigan 2800 Plymouth Rd. Ann Arbor. MI 48109 Tel: +1-734-998-7500 Fax: +1-734-998-7711 oberen@med.umich.edu.
*contributed equally

Conflict of Interest Disclosures: None.

Conclusions—In the sheep transition from paroxysmal to persistent AF shows continuous LA-to-RA DF gradients in-vivo together with enlargement of the PLA, which harbors the highest frequency domains and patterns of activation compatible with drifting rotors.

Keywords

atrial fibrillation; electrophysiology mapping; remodeling; dominant frequency; rotors

Introduction

Atrial fibrillation (AF) is the most common sustained arrhythmia in clinical practice.[1] When the arrhythmia lasts continuously >7 days it is designated as persistent. Spontaneous, pharmacological or ablative resumption of sinus rhythm becomes infrequent as the arrhythmia lasts >1 year, termed permanent AF.[2]

Experimental studies using high-resolution optical mapping have shown that acute AF often depends on discrete drivers or rotors generating relatively periodic and organized activity in the form of spiral waves that spin at high frequency around a functional core.[3] The waves emanating from such rotors interact with anatomic and functional obstacles in their path, giving rise to fibrillatory conduction and establishing a spatially distributed hierarchical organization in the local dominant frequencies (DF) of atria.[4] Thus, spectral analysis in animal[3] and human[5] paroxysmal AF demonstrating maximal DF (DF_{max}) at or near the pulmonary veins (PVs) and gradients toward the left and right atria (LA and RA), also demonstrated a co-localization of sources and DF_{max} sites. The DF_{max} has been suggested to provide both mechanistic and ablative guidance; the presence of a LA-to-RA DF_{max} gradient and its eradication by radiofrequency ablation predicts long-term freedom from both paroxysmal and persistent AF.[6]

The atria of persistent AF patients have a more widespread distribution of DF_{max}, mainly outside the PVs region, and higher DF_{max} values than paroxysmal AF patients.[6, 7] Studies on persistent AF have attributed the acceleration of the atrial activation rate to atrial remodeling in both animals[8] and humans.[9] However, those studies were somehow limited by the fact that they addressed persistent AF of relatively short[8] or unconfirmed, duration.[10, 11] In addition, no information was provided on the spatial distribution of the atrial activation rates. Here we aimed at filling those gaps by studying *in-vivo* the time-course of the changes in DF values and the evolution of the left-to-right DF dispersion during the transition from paroxysmal to persistent AF.

Using a chronic RA tachypacing model of persistent AF in the sheep, along with continuous cardiac rhythm monitoring by dual implantable devices, we tested the hypothesis that *in-vivo* DF values during AF progressively increase while preserving in the long-term a DF difference between LA and RA. Mapping of the atria and subsequent structural analyses *ex-vivo* confirmed the presence of DF gradients from posterior LA (PLA) to RA, together with patterns of activation consistent with the contention that drifting rotors in an enlarged PLA may underlie AF dynamics in this model.

Methods

Induction of Persistent AF

All procedures were approved by the University of Michigan Committee on Use and Care of Animals and complied with National Institutes of Health guidelines. Eight 6–8 month-old sheep (≈40 Kg) were used for implantation. Anesthesia was induced using propofol (4–6 mg/kg IV), and maintained by isoflurane inhalation. A bipolar lead was inserted into the RA appendage (RAA) through the left external jugular vein. The proximal end of the lead was screwed to the sterile pacemaker (Victory® XLDR, St. Jude Medical. Sylmar, CA. USA), which was sheltered in a subcutaneous pouch. Thereafter, an implantable loop recorder (ILR, Reveal® XT, Medtronic, Inc. Minneapolis, MN. USA) was placed subcutaneously on the left side of the sternum in close proximity to LA (Figure 1A, B). Based on fluoroscopy images a distance of about 2 cm between the ILR and the LA free wall was confirmed and guaranteed that it was opposing the RAA lead location and recorded primarily LA activity. We obtained left ventricular ejection fraction (LVEF) measurements at implantation and before euthanasia by transthoracic echocardiography (Sonos 5500, Hewlett-Packard, Palo Alto, CA) using a long-axis parasternal view (Supplemental Figure 5).

After 10 days of recovery, the pacemaker was programmed to induce AF by fast atrial pacing with an algorithm consisting of 30-sec pacing at 20 Hz followed by 10-sec sensing. The ILR was programmed to identify AF episodes lasting >6 sec during the 10-sec sensing. The pacemaker and ILR were interrogated weekly during the study period, including automatic registration of detected AF events by the ILR when available. The duration in weeks until the first self-sustained AF episode (>6 sec in duration, see Figure 1C) was quantified for each animal, after which weekly monitoring confirmed the maintenance of AF.

To generate a clinically relevant persistent AF model, we stopped the pacing algorithm at the end of the follow-up period between 9–24 weeks. Persistent AF was defined based on the criteria used for human AF as those episodes lasting >7 days upon switching off the fast pacing program (Figure 1D). Episodes lasting ≤7 days were considered paroxysmal AF.[2]

In-vivo Determination of DF

Data acquisition—Two electrograms were simultaneously obtained during the *in-vivo* protocol: (i) RAA lead tip electrograms with a case reference were exported at a sampling rate of 512 Hz, and (ii) ILR recorded single lead electrograms were exported as a vector PDF file, which was magnified 1200% and then digitized in the Matlab (MathWorks, Natick MA) environment. The digitized signal was then superimposed on the original electrogram image for visual inspection to ensure quality data. The time scale (effective sample rate acquisition) was calculated for each trace individually based on average distance between gridline centers in the vector PDF file.

Data processing—Recordings obtained by the ILR, whose canister was external to the LA, contained a mixture of atrial and ventricular activity. To analyze the atrial activity, the ventricular activity (dubbed QRST) was subtracted from the original recordings. To enhance

confidence in the QRST removal 2 single-lead QRST removal algorithms were used: (i) A principal component analysis based AF estimation[12] (PCA) and (ii) An adaptive singular value QRST cancellation[13] (SVC). After QRST removal, a bias-free bidirectional Butterworth bandpass filter (4–35 Hz) was applied to each trace. The fast Fourier transform (FFT) was then used to obtain the DF in 5 sec-long signals from the ILR and RAA electrograms. Finally, DF values from RAA and ILR electrograms were compared to identify *in-vivo* differences between the two regions (see Supplemental Methods and Supplemental Figures 1–4 for details).

Evaluation of Ventricular Activity Removal

To further validate the methods for QRST removal, performance was evaluated against a set of synthesized time-series test cases constructed with a known reference atrial and ventricular activity that was obtained from the animals studied. Each test case was constructed by adding a selected set of QRST complexes to a 5 sec-long episode of atrial-only activity extracted and spliced manually from the original electrograms. The effective heart rate was set for the average heart rate of the sheep during the study (≈100 bpm). Test cases were grouped according to the morphological variability between QRST complexes as measured by the Pearson correlation index.

Mapping of Isolated Hearts

Five sheep (≈66 Kg) underwent 20–24 weeks of continuous tachypacing induced AF. Hearts were removed via thoracotomy and connected to a Langendorff-perfusion system with re-circulating oxygenated (95% O_2, 5% CO_2) Tyrode's solution.

The experiments were performed under constant intra-atrial pressure to subthreshold AF-inducing level of 5 cm H_2O, resembling the diastolic LA pressure.[14] Tetrapolar electrode catheters were placed in each of the PVs. Two additional custom-made bipolar electrodes were placed on the top of the RAA and LA appendage (LAA; Figure 1E). Epicardial and endocardial optical mapping (Di-4-ANEPPS 5–10 mg/mL) of the LAA and PLA, respectively, were performed simultaneously as described elsewhere (See Figure 1E, F and Supplemental Methods).[15]

AF and DF Analysis in Isolated Hearts

Spontaneous AF in the Langendorff-perfused hearts was allowed to continue uninterrupted for 50 minutes. Five sec-long optical movies were acquired at 2 min intervals. Acquisition of the optical movies triggered simultaneous acquisition of the bipolar recordings.

DF maps were obtained from each optical movie after applying a FFT to the fluorescence signal time-series recorded at each pixel (Figure 1F). FFT was also applied to the 5-sec bipolar signals following 4–35 Hz band-pass filters. In the PLA, waves were tracked for outward and inward directionality at 10-min intervals using phase movies constructed by means of Hilbert transformation.[16] Patterns of activation were classified as rotors and breakthroughs as described elsewhere.[15]

Structural Changes in Persistent AF

Hearts preserved in 10% neutral buffered formalin from AF animals (N=7) and body weight-matched controls (N=4) were used to quantified the area of the PLA and determine changes in interstitial fibrosis as described in the Supplemental Methods.

Statistical Analyses

Data are reported as mean±SEM except where noted. Normal distribution of variables was assessed with Shapiro-Wilk test. A mixed regression model has been applied to multiple group analyses and repeated measurements data. The Mann-Whitney U test was used to compare the PLA area in AF animals versus weight-matched controls and to assess differences in the degree of atrial fibrosis. *Post hoc* comparisons were corrected by Bonferroni test when appropriate. $p<0.05$ was considered statistically significant.

Results

DF Increases after the First AF Episode

Traces stored in the memory of the lLR were carefully analyzed during weekly interrogations to search for the presence of AF and its DF. As shown in Figure 2A, the time for detection of the first AF episode varied considerably between 5 and 60 days (median 14, normality by Shapiro-Wilk test; $p=0.05$) of tachypacing. Using the ILR AF detection ability we identified first-time self-sustained AF in 6 episodes. In Figure 2B, we show a progressive increase in DF values from 7±0.21 to 9.9±0.31 Hz ($N=6$, $p<0.05$) during the first 2 weeks, after which the DF remained stable for the duration of the follow-up period. The first AF episode was considered as the zero reference point. Sample data from the ILR and RAA lead at week 1 and week 14 are shown in panels C and D. The PCA method was used for QRST removal in the ILR signal based on best performance analysis over larger range of QRST variability (see Methods and Supplemental Figures 6 and 7). After 14 weeks under tachypacing induced AF the power spectra showed an increase in DF in both ILR (7.5 to 10.25 Hz) and RAA lead traces (7.25 to 8.75 Hz).

In-vivo Long-Term Left-to-Right DF Differences

Once AF was detected for the first time, DF values obtained from the ILR and the RAA lead were determined weekly and analyzed. One sheep with a 9-week follow-up was excluded, since only traces from the ILR were available. The DF value for each week and animal was determined as the mode DF (the most commonly occurring) in a median of 5 ILR (range 2 to 8) and 34 RAA lead (range 3 to 327) episodes of 5-sec long signal each. In Figure 3A and 3B, the spectrograms obtained from a sample animal show a progressive increase in the DF of the average power spectra (Welch method) of the traces for a given week, across the 14-week period. The ILR consistently recorded significantly higher overall average DFs compared to the RAA lead (9.4±0.21 vs. 8.4±0.22 Hz, respectively, $p=0.002$). In Figure 3C, the cumulative plot for all the animals shows that the DF values in the ILR (red) remain 1.3±0.1 Hz higher than the RAA values (blue) for up to 22 weeks. Time and again, the ILR detected higher DF values than those detected by the RAA lead (10.6±0.08 vs. 9.3±0.1 Hz,

respectively. p<0.0001. Figure 3D) over the entire period of recording. The results suggest the presence of long-term persistent high frequency sources in the LA.

Optically Mapped Isolated Hearts

Spontaneous AF was present in each of the explanted hearts (N=5) upon Langendorff perfusion. The time-course of the DF_{max} on the PLA and RAA of each heart is shown in Figure 4A over a 50 min period of spontaneous AF. Visual examination of the DF_{max} data reveals variations between hearts and between the PLA and RAA, with temporal fluctuations, but without a trend. In figure 4B we present the mean regional DF_{max} values during the entire 50 min of self-sustained AF for the PLA, LAA and RAA, either optically mapped or electrically recorded. The global DF_{max} was consistently localized at the PLA with a statistically significant DF gradient from PLA to LAA and RAA (9.1±1.0 vs. 7.9±0.7 and 6.9±0.9 Hz, respectively, p<0.05).

In addition, *in-vivo* DF values from the ILR were compared to DF_{max} in the Langendorff-perfused hearts. Figure 4C shows lower DF_{max} in the isolated hearts (9.1±0.2 vs. 10.6±0.1 Hz. p<0.0001), which might be explained by autonomic denervation.

To further establish the patterns of activation underlying the DF_{max} values in the PLA we used phase movies to compare the number of waves leaving versus entering the mapped PLA region (1 sec-long segments). In Figure 5A, data from 5 hearts at 10 min intervals demonstrate that the number of waves propagating outward consistently exceeded those propagating inward (6.6±0.2 vs 2.9±0.2 respectively, p<0.05). Panel B shows examples of outward (bottom left)/inward (bottom right) propagation from/toward the field of view on the PLA (top). In addition, rotors and breakthroughs in the PLA were analyzed by counting the total number of rotations/cm^2 (regardless of lifespan of rotors) and breakthroughs/cm^2 in 2 sec-long segments. Figure 5C shows at 10 min intervals a significantly higher number of breakthroughs/cm^2 compared to rotations/cm^2 in the mapped PLA.

Whether those breakthroughs are the surface expression of intramural reentrant activity or focal activity can be assessed by movies such as Supplemental Movie 1 and the snapshots of Figure 5D, in which a rotor with its filament perpendicular to the field of view drifts from the PLA towards the LAA. As soon as the rotor enters in the LAA field of view, the patterns of activation switch from breakthroughs to reentry and the drifting rotor becomes the main source driving the AF. Concomitant transition in the DF_{max} values from the PLA to the LAA when the rotor appears in the field of view of the LAA further confirm the essential role of rotors in this persistent AF model.

Structural Changes and the Persistence of AF

Using the clinical classification of persistent AF would require episodes to last >7 days without artificial intervention by the pacemaker.[2] However, the transition into such condition may vary considerably from one animal to another as was shown for AF induction (Figure 2A). Although all animals developed self-sustained AF during intermittent fast atrial pacing, 2 out of 7 did not develop persistent AF after stopping the pacing protocol (Supplemental Figure 8A). Two representative examples are shown in Supplemental Figure

8; whereas in one animal the AF lasted >7 days after the pacing program was switched off (panel B), in the other one spontaneous AF termination was observed 3 days after the pacing program was stopped (panel C).

DF values measured on the ILR (N=7) during the last week before the offset of tachypacing were not significantly different when comparing persistent AF versus non-persistent AF animals (10.0±0.8 vs. 10.0±2.1, respectively, p=0.67). Therefore, additional factors other than the increase in DF values must be involved in the progressive development of the arrhythmia. As shown in Figure 6, sectioning of the LA and quantification of the endocardial side of the PLA area (panel A) demonstrates that long-term tachypacing induced AF animals (N=7) have a significantly enlarged PLA area compared to body weight-matched controls (N=4) (7.48±0.25 vs 5.96±0.29 cm^2, p=0.006, Figure 6B). However, as presented in Supplemental Figure 9A, fibrosis quantification on images obtained from slices stained with Picrosirius red did not show significant increase in fibrosis in any of the sectioned areas compared to weight-matched controls. Additional sectioning in the LA areas and staining using Masson's trichrome further confirmed those results (Supplemental Figure 9B).

Development of atrial fibrosis is well established in AF models associated to congestive heart failure.[17] Conversely, predominant electrical remodeling with minimal or no changes in atrial fibrosis is present in tachypacing induced AF models even after long periods of fast pacing, as long as tachycardimyopathy is not present.[18] Echocardiographic data at baseline and before euthanasia showed that the LVEF was preserved (57±1.4 to 55±0.7%, respectively) in all animals studied (Supplemental Table 1). In addition, the average heart rate during the follow up remained within the upper normal limit in sheep (99 bpm, Supplemental Table 1), which makes the development of tachycardiomyopathy very unlikely.

Discussion

We have used a sheep model of persistent AF induced by intermittent atrial tachypacing in which we monitored on a weekly basis the time-course of the DF in the ILR (in close proximity to LA) and the RA. The results show a progressive spontaneous increase in DF over a 2-week period after the first detected AF episode, suggesting electrical remodeling secondary to AF. Most important, a consistent LA-vs-RA DF difference lasting more than 22 weeks in most animals correlated with the presence of rotors, DF gradients, and outward propagation from the PLA during sustained AF in the explanted, Langendorff-perfused hearts. . While in this model interstitial fibrosis does not significantly increase, atrial structural changes leading to PLA enlargement may make rotors less likely to collide with anatomical boundaries, thus contributing to the persistence of the arrhythmia. On the other hand, changes in subcellular structures such as the ryanodine receptor, may have led to sarcoplasmic reticulum Ca^{2+} leak and contributed to AF persistence by increasing triggered activity, dispersion of refractoriness or promoting reentry initiation.[19] Altogether, our data support the contention that drifting transmural and intramural rotors may drive the highest frequency activity detected in the PLA.

Temporal criteria for persistent AF are well defined in the clinical setting.[2] However, persistent AF in animal models has not been rigorously defined, which may have led to inconsistencies in the results reported for models versus patients with persistent AF.[8, 10] Fast atrial pacing is a common approach to induce AF in animal models. Yet, some studies use the term "persistent AF" for those episodes in which the arrhythmia sustains in the short term (<7 days) in the absence of pacing,[8, 10] either for cardioversion attempts or electrophysiological measurements.[11, 20] Although spontaneous termination has been observed after 4 weeks of tachypacing induced AF in chronically instrumented goats,[21] cases of AF have also been defined as long-lasting when they sustain for few days after rapid atrial pacing.[21] In the current study most of animals developed persistent AF lasting >1 week, thus the time-course of the DF and its left-to-right gradient we quantify is highly relevant to the progression of a clinical-like persistent AF.

Implications of Left-to-Right DF Gradients in Persistent AF

Although few data clearly demonstrate the presence of left-to-right DF gradients in patients with persistent and permanent AF, Sahadevan et al,[22] using epicardial mapping during cardiac surgery, have demonstrated the presence of rapid and regular rhythms mainly located at the LA in 7 out of 9 patients with persistent/permanent AF. The cycle length of the rapid and regular rhythm areas was shorter than that of the areas with irregular activation. Atienza et al[6] have shown that left-to-right DF gradients were present in 84% of patients with persistent AF. Furthermore, persistent AF patients remained AF-free on follow-up when ablation significantly reduced DF_{max} in the LA and RA, abolishing the LA-to-RA DF gradient. Similarly, in a larger population of patients with long-lasting persistent AF, Hocini et al[23] have observed that in some cases of AF ablation a right-to-left frequency gradient appeared after prolongation of the AF LA cycle length. RA ablation terminated AF in 55% of those patients. Interestingly, those patients had longer AF duration and larger RA diameter. Somehow, our model resembles early stages of clinical persistent AF, in which the LA-to-RA gradient is still present and organized period activity is identified in the PLA giving raise to fibrillatory conduction towards the rest of the atria. Longer periods in AF might eventually increase the fibrosis quantification and make other areas of the atria suitable for harboring reentrant sources.

Mechanism Underlying the DF_{max} in Persistent AF

Electrical remodeling and functional changes in subcellular structures lead to both abbreviation of atrial action potential duration and refractory period,[11] and increase susceptibility to Ca^{+2}-dependent triggered activity,[19] altogether promoting reentry. However, whether random fibrillatory waves, triggered activity or highly organized 3D reentrant sources are the underlying mechanism of persistent AF is controversial. Data from patients with persistent AF that underwent cardiac surgery and electrical epicardial mapping in LA, RA and PLA, show the presence of non-repetitive epicardial breakthroughs more frequently occurring in the PV area compared to RA and LA.[24] Although those results might suggest the presence of fibrillation waves propagating in deeper layers of the atrial wall. Important limitations such as sequential and exclusive epicardial mapping precludes ruling out the presence of endocardial/intramural reentrant sources giving raise to epicardial breakthroughs. In addition, the lack of simultaneous recording of Ca^{+2} transients prevents us

from ruling out the possibility that the epicardial breakthroughs were caused by triggered activity.[19] Similarly, our study also identifies higher number of breakthroughs compared to rotors in the PLA. However, direct visualization of the endocardial side of the PLA, simultaneous mapping of PLA-LAA and much higher mapping resolution (≈0.23 mm^2/pixel) than the conventional multi-electrodes arrays allowed the demonstration of a rotor drifting toward the LAA with its center of rotation oriented perpendicular to the field of view; an apparent breakthrough pattern before the rotor enters, turns to a rotor pattern when the rotor is visible. Concomitant changes in the DF_{max} values from PLA to LAA upon entering the rotor further support the essential role of rotors in maintain persistent AF. The latter also makes Ca^{+2}-dependent triggered activity more likely to be related to reentry initiation rather than maintenance of the arrhythmia.

Limitations

In-vivo LA-to-RA DF differences were obtained from only two single-lead traces, which limit the ability to characterize the spatial distribution of the DF values across the atria. In addition, the lack of synchronization of *in-vivo* recordings prevented an *in-vivo* directionality analysis. Atrial activity obtained from the ILR may be considered more global than that recorded by the intracardial lead. However, as shown in Figure 1B, the close proximity of the ILR to the LA of the sheep and the confirmation of the DF_{max} at the PLA in optically mapped hearts, supports the results obtained from the ILR traces.

Fibrosis quantification was performed in preserved hearts after optical mapping, which is not clear whether or not is affecting Picrosirius red staining. Additional sectioning and staining using Masson's trichrome reproduced similar results, which reduces likelihood for biased estimation of the fibrosis.

Finally, cellular and ionic remodeling underlying AF initiation, rotor activity and DF gradients have not been investigated in this study due to incompatibility with the optical mapping of the entire heart. Importantly, the DF gradients observed in this persistent AF model cannot be extrapolated to longer periods of AF such as permanent AF, in which stronger structural remodeling may be involved and left-to-right gradients may decrease.[6]

Conclusions

Time-course analysis of *in-vivo* AF in sheep shows an initial 2-week period of progressive increase in DF followed by DFs stabilization for up to 24 weeks thereafter. The different long-term DFs in the ILR and the RA recorded *in-vivo*, together with DF gradients and patterns of activation in the optically mapped explanted hearts, strongly suggest the presence of long-lasting AF reentrants drivers located at the PLA in this model of persistent AF.

Supplementary Material

Refer to Web version on PubMed Central for supplementary material.

Acknowledgments

We thank Andreu Climent and María Guillém for assistance in signal processing. We also thank Gail Rising and Krishna Bandaru for technical assistance, and Rosario Madero for assistance in statistical analyses. We thank St Jude Medical and Medtronic for assistance with implantable devices.

Funding Sources: This work was supported in part by National Heart, Lung, and Blood Institute Grants (P01-HL039707 and P01-HL087226 to JJ and OB), the Leducq Foundation and CNIC (JJ and OB), the University of Michigan Gelman/Innovation and Coulter Awards (OB), St. Jude Medical Grant (JJ, OB, JK) a Spanish Society of Cardiology Fellowship, the Alfonso Martín Escudero Foundation (DFR), and the Fédération Française de Cardiologie (RPM).

References

1. Kannel WB, Wolf PA, Benjamin EJ, Levy D. Prevalence, incidence, prognosis, and predisposing conditions for atrial fibrillation: Population-based estimates. Am J Cardiol. 1998; 82:2N–9N.
2. Camm AJ, Kirchhof P, Lip GY, Schotten U, Savelieva I, Ernst S, Van Gelder IC, Al-Attar N, Hindricks G, Prendergast B, Heidbuchel H, Alfieri O, Angelini A, Atar D, Colonna P, De Caterina R, De Sutter J, Goette A, Gorenek B, Heldal M, Hohloser SH, Kolh P, Le Heuzey JY, Ponikowski P, Rutten FH, Vahanian A, Auricchio A, Bax J, Ceconi C, Dean V, Filippatos G, Funck-Brentano C, Hobbs R, Kearney P, McDonagh T, Popescu BA, Reiner Z, Sechtem U, Sirnes PA, Tendera M, Vardas PE, Widimsky P, Agladze V, Aliot E, Balabanski T, Blomstrom-Lundqvist C, Capucci A, Crijns H, Dahlof B, Folliguet T, Glikson M, Goethals M, Gulba DC, Ho SY, Klautz RJ, Kose S, McMurray J, Perrone Filardi P, Raatikainen P, Salvador MJ, Schalij MJ, Shpektor A, Sousa J, Stepinska J, Uuetoa H, Zamorano JL, Zupan I. Guidelines for the management of atrial fibrillation: The task force for the management of atrial fibrillation of the european society of cardiology (esc). Europace. 2010; 12:1360–1420. [PubMed: 20876603]
3. Mandapati R, Skanes A, Chen J, Berenfeld O, Jalife J. Stable microreentrant sources as a mechanism of atrial fibrillation in the isolated sheep heart. Circulation. 2000; 101:194–199. [PubMed: 10637208]
4. Mansour M, Mandapati R, Berenfeld O, Chen J, Samie FH, Jalife J. Left-to-right gradient of atrial frequencies during acute atrial fibrillation in the isolated sheep heart. Circulation. 2001; 103:2631–2636. [PubMed: 11382735]
5. Atienza F, Almendral J, Moreno J, Vaidyanathan R, Talkachou A, Kalifa J, Arenal A, Villacastin JP, Torrecilla EG, Sanchez A, Ploutz-Snyder R, Jalife J, Berenfeld O. Activation of inward rectifier potassium channels accelerates atrial fibrillation in humans: Evidence for a reentrant mechanism. Circulation. 2006; 114:2434–2442. [PubMed: 17101853]
6. Atienza F, Almendral J, Jalife J, Zlochiver S, Ploutz-Snyder R, Torrecilla EG, Arenal A, Kalifa J, Fernandez-Aviles F, Berenfeld O. Real-time dominant frequency mapping and ablation of dominant frequency sites in atrial fibrillation with left-to-right frequency gradients predicts long-term maintenance of sinus rhythm. Heart Rhythm. 2009; 6:33–40. [PubMed: 19121797]
7. Yoshida K, Ulfarsson M, Oral H, Crawford T, Good E, Jongnarangsin K, Bogun F, Pelosi F, Jalife J, Morady F, Chugh A. Left atrial pressure and dominant frequency of atrial fibrillation in humans. Heart rhythm. 2011; 8:181–187. [PubMed: 21034858]
8. Anne W, Willems R, Holemans P, Beckers F, Roskams T, Lenaerts I, Ector H, Heidbuchel H. Self-terminating af depends on electrical remodeling while persistent af depends on additional structural changes in a rapid atrially paced sheep model. J Mol Cell Cardiol. 2007; 43:148–158. [PubMed: 17597147]
9. Voigt N, Trausch A, Knaut M, Matschke K, Varro A, Van Wagoner DR, Nattel S, Ravens U, Dobrev D. Left-to-right atrial inward rectifier potassium current gradients in patients with paroxysmal versus chronic atrial fibrillation. Circ Arrhythm Electrophysiol. 2010; 3:472–480. [PubMed: 20657029]
10. Roka A, Toth E, Szilagyi S, Merkely B. Electrical atrial fibrillation induction affects the characteristics of induced arrhythmia. J Electrocardiol. 2008; 41:131–137. [PubMed: 17631892]
11. Yue L, Feng J, Gaspo R, Li GR, Wang Z, Nattel S. Ionic remodeling underlying action potential changes in a canine model of atrial fibrillation. Circ Res. 1997; 81:512–525. [PubMed: 9314832]

12. Castells F, Mora C, Rieta JJ, Moratal-Perez D, Millet J. Estimation of atrial fibrillatory wave from single-lead atrial fibrillation electrocardiograms using principal component analysis concepts. Med Biol Eng Comput. 2005; 43:557–560. [PubMed: 16411627]
13. Alcaraz R, Rieta JJ. Adaptive singular value cancelation of ventricular activity in single-lead atrial fibrillation electrocardiograms. Physiol Meas. 2008; 29:1351–1369. [PubMed: 18946157]
14. Schotten U, de Haan S, Neuberger HR, Eijsbouts S, Blaauw Y, Tieleman R, Allessie M. Loss of atrial contractility is primary cause of atrial dilatation during first days of atrial fibrillation. Am J Physiol Heart Circ Physiol. 2004; 287:H2324–2331. [PubMed: 15256374]
15. Filgueiras-Rama D, Martins RP, Ennis SR, Mironov S, Jiang J, Yamazaki M, Kalifa J, me, Jalife J, Berenfeld O. High-resolution endocardial and epicardial optical mapping in a sheep model of stretch-induced atrial fibrillation. J Vis Exp. 2011:e3103.
16. Warren M, Guha PK, Berenfeld O, Zaitsev A, Anumonwo JM, Dhamoon AS, Bagwe S, Taffet SM, Jalife J. Blockade of the inward rectifying potassium current terminates ventricular fibrillation in the guinea pig heart. J Cardiovasc Electrophysiol. 2003; 14:621–631. [PubMed: 12875424]
17. Li D, Fareh S, Leung TK, Nattel S. Promotion of atrial fibrillation by heart failure in dogs: Atrial remodeling of a different sort. Circulation. 1999; 100:87–95. [PubMed: 10393686]
18. Ausma J, Wijffels M, Thone F, Wouters L, Allessie M, Borgers M. Structural changes of atrial myocardium due to sustained atrial fibrillation in the goat. Circulation. 1997; 96:3157–3163. [PubMed: 9386188]
19. Voigt N, Li N, Wang Q, Wang W, Trafford AW, Abu-Taha I, Sun Q, Wieland T, Ravens U, Nattel S, Wehrens XH, Dobrev D. Enhanced sarcoplasmic reticulum ca2+ leak and increased na+-ca2+ exchanger function underlie delayed afterdepolarizations in patients with chronic atrial fibrillation. Circulation. 2012; 125:2059–2070. [PubMed: 22456474]
20. Nishida K, Sarrazin JF, Fujiki A, Oral H, Inoue H, Morady F, Nattel S. Roles of the left atrial roof and pulmonary veins in the anatomic substrate for persistent atrial fibrillation and ablation in a canine model. J Am Coll Cardiol. 2010; 56:1728–1736. [PubMed: 21070924]
21. Wijffels MC, Kirchhof CJ, Dorland R, Allessie MA. Atrial fibrillation begets atrial fibrillation. A study in awake chronically instrumented goats. Circulation. 1995; 92:1954–1968. [PubMed: 7671380]
22. Sahadevan J, Ryu K, Peltz L, Khrestian CM, Stewart RW, Markowitz AH, Waldo AL. Epicardial mapping of chronic atrial fibrillation in patients: Preliminary observations. Circulation. 2004; 110:3293–3299. [PubMed: 15520305]
23. Hocini M, Nault I, Wright M, Veenhuyzen G, Narayan SM, Jais P, Lim KT, Knecht S, Matsuo S, Forclaz A, Miyazaki S, Jadidi A, O'Neill MD, Sacher F, Clementy J, Haissaguerre M. Disparate evolution of right and left atrial rate during ablation of long-lasting persistent atrial fibrillation. J Am Coll Cardiol. 2010; 55:1007–1016. [PubMed: 20202517]
24. de Groot NM, Houben RP, Smeets JL, Boersma E, Schotten U, Schalij MJ, Crijns H, Allessie MA. Electropathological substrate of longstanding persistent atrial fibrillation in patients with structural heart disease: Epicardial breakthrough. Circulation. 2010; 122:1674–1682. [PubMed: 20937979]

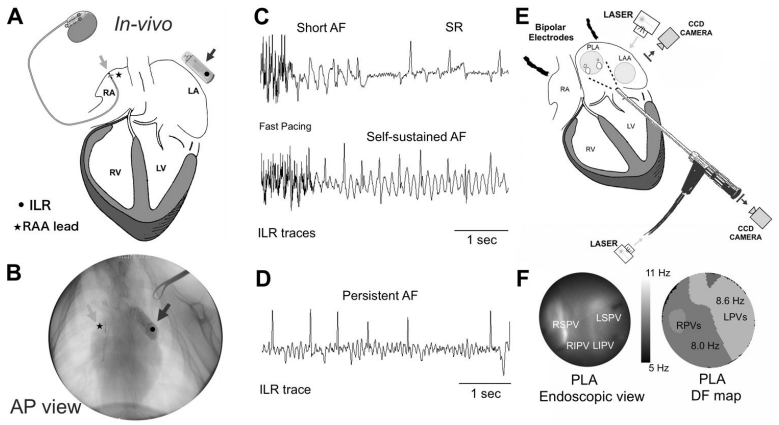

Figure 1.

In-vivo and *ex-vivo* model, protocols and mapping experiments. **A)** A diagram of a pacemaker with the lead in the RAA (light grey arrow) and ILR (dark grey arrow) close to the LA. **B)** Fluoroscopic view of the lead in the RAA (light grey arrow) and the ILR next to the LA (dark grey arrow). **C)** ILR traces at different stages of the persistent AF protocol. Rapid pacing appears at the beginning of the trace. **D)** A 6-sec long AF episode during AF that persisted for >7 days after turning off the fast pacing. **E)** *Ex-vivo* Epicardial and endocardial mapping setup includes synchronized dual CCD cameras as well as bipolar electrodes placed in the RA and the roof of the LA. Bipolar signals are also obtained from the pulmonary veins. **F)** Endoscopic view of the PLA (left) and DF map during AF.

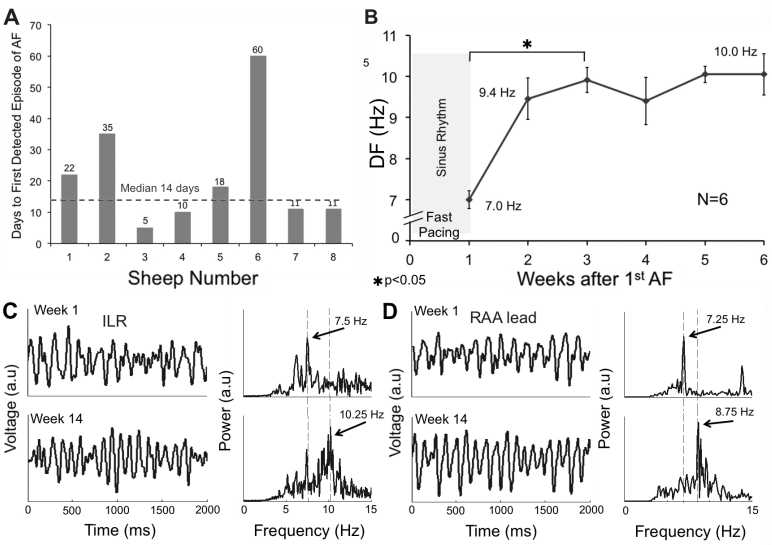

Figure 2.

Heterogeneous onset of AF and its acceleration. **A)** Number of weeks of tachypacing before any AF episode is detected in sheep sorted by sequential implantation order. **B)** DF values from the ILR traces show an increase in DF over a 2-week period after the first tachypacing induced AF episode. **C)** AF traces and corresponding power spectra obtained from the ILR after QRST removal and filtering. DF increases from 7.5 to 10.25 Hz from week 1 to week 14, respectively. **D)** RAA lead traces and corresponding power spectra. DF increases from 7.25 to 8.75 Hz during the same period.

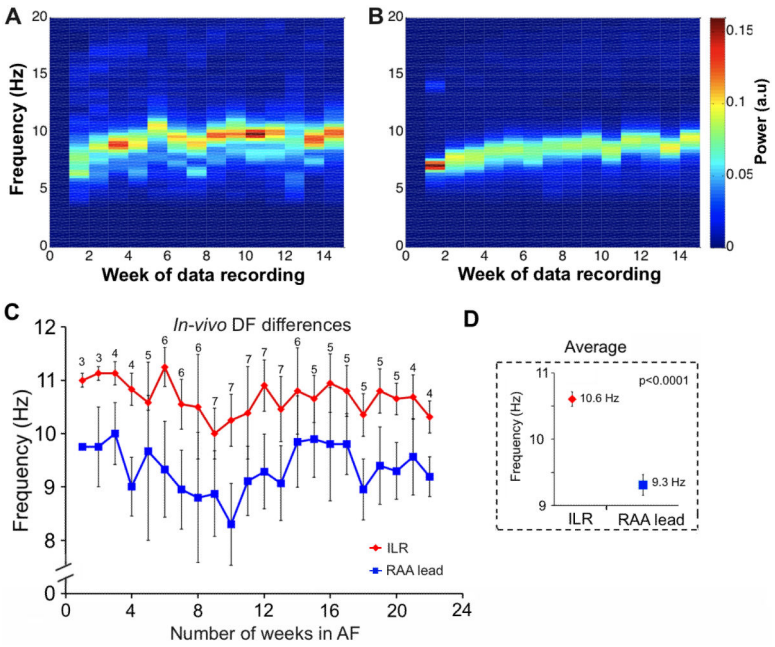

Figure 3.

Left-to-right DF differences *in-vivo*. **A** and **B)** Spectrograms generated from the ILR and RAA lead signals, respectively, in a sample animal. The average power spectra (Welch method) of the traces for a given week shows a progressive increase in DF (14 weeks are shown). **C** and **D)** DF values obtained from the ILR (red symbols) are significantly higher than those obtained from the RAA lead; 22 weeks of follow up are shown.

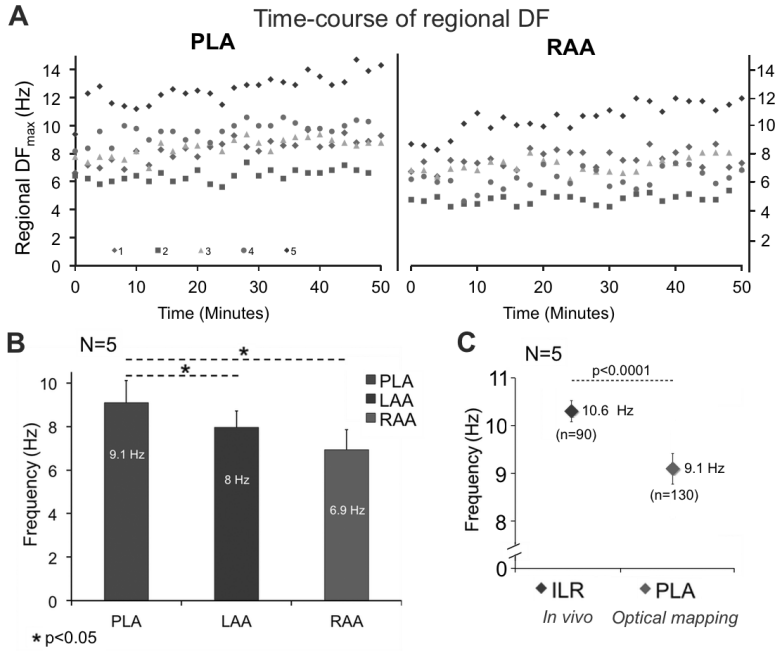

Figure 4.

A) Time-course of DF in 5 isolated hearts over a 50 min period (each color represents one heart). The DF_{max} was consistently localized in the PLA. **B)** Statistically significant DF gradient from PLA to LAA-RAA. **C)** *In-vivo* mean DF_{max} from the ILR was significantly different from mean DF_{max} at the PLA (10.6±0.1 vs. 9.1±0.2 Hz. p<0.0001). `N' represents the number of animals and `n' the total number of measurements.

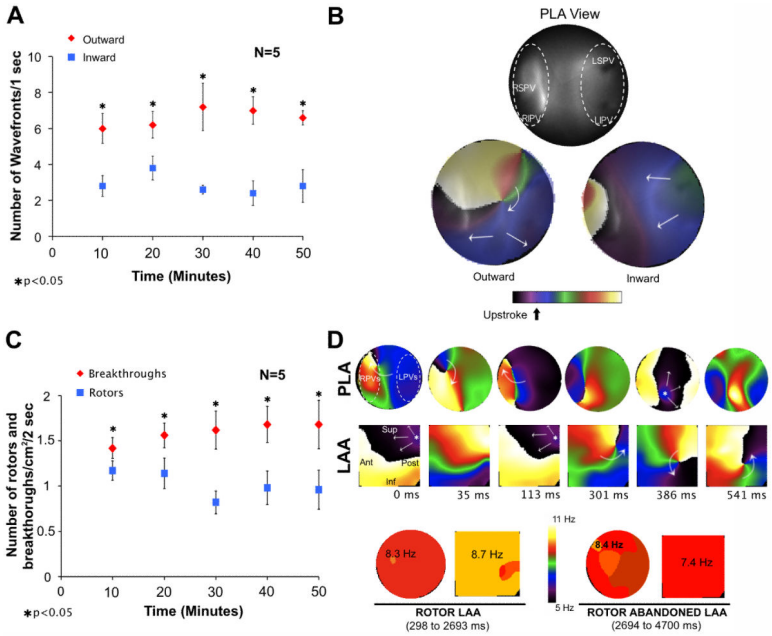

Figure 5.

Patterns of activation in the PLA of isolated hearts during AF. A) The graph shows that the number of outwardly propagating wavefronts/sec was significantly larger than the number of inwardly propagating wavefronts/sec. B) Top, optical field on the endocardium of the PLA; bottom, snapshots of phase movies showing a rotor generating outwardly propagating waves (left). An inwardly propagating wave is shown on the right. C) The number of breakthroughs/cm^2/2-sec is higher than the number of rotors/cm^2/2-sec. D) Top, snapshots from a phase movie show a rotor appearing in the field of view of the LAA. The patterns of activation switch from breakthroughs (0-to-113 ms) to a meandering rotor (301-to-541 ms). Bottom, the DF_{max} is in the LAA when the rotor stays in the field of view and go back to PLA when the rotor drifts outside the LAA.

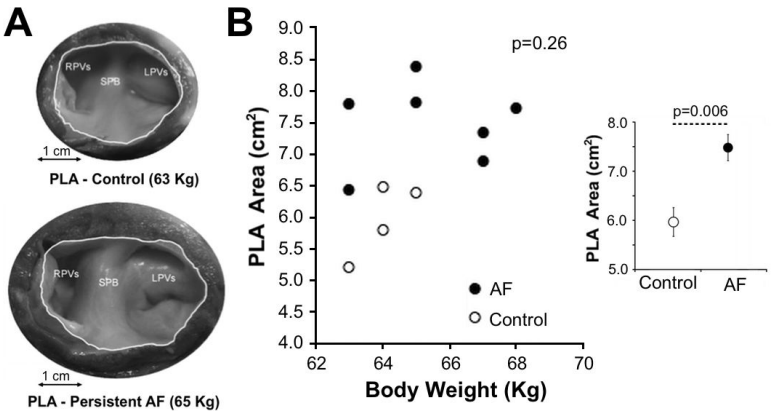

Figure 6.

Enlargement of the PLA area in sheep with AF. **A)** Macroscopic images of the endocardial side of the PLA area in a persistent AF sheep (bottom) and weight-matched control (top). **B)** No significant correlation between body weight and PLA area was observed (Spearman's test). Inset: On average, AF sheep show a significantly larger PLA area compared to weight-matched controls (Mann-Whitney U test).